Propagation of axially symmetric flattened Gaussian beams

V. Bagini, R. Borghi, F. Gori, A. M. Pacileo, and M. Santarsiero

Dipartimento di Fisica, Università La Sapienza, Piazzale Aldo Moro 2, 00185 Rome, Italy

D. Ambrosini and G. Schirripa Spagnolo

Dipartimento di Energetica, Università dell'Aquila, Monteluco di Roio, 67040 Roio Poggio (AQ), Italy

Received October 16, 1995; accepted December 7, 1995; revised manuscript received January 23, 1996

Flattened Gaussian beams are characterized by a waist profile that passes in a continuous way from a nearly flat illuminated region to darkness. The steepness of the transition region is controlled by an integer parameter N representing the order of the beam. Being expressible as a sum of N Laguerre–Gauss modes, a flattened Gaussian beam turns out to be very simple to study as far as propagation is concerned. We investigate the main features of the field distribution pertaining to a flattened Gaussian beam throughout the space and present experimental results relating to the laboratory production of this type of beam. © 1996 Optical Society of America

1. INTRODUCTION

In many applications of light beams, a field is required whose amplitude on a fixed plane is as uniform as possible within a certain area and practically vanishing outside. Typical examples are furnished by optical processing, beam shaping, and laser cavities.[1–9] The strictly uniform case with abrupt transition to zero, i.e., the case in which the field profile is a circ function,[10] is rather inconvenient. In fact, ringing phenomena, well known from the study of diffraction of a plane wave by a circular hole, are exhibited in the course of propagation. In addition, the evaluation of the propagated field cannot be performed in a closed form, and one has to resort to numerical methods.[11–13] To reduce ringing effects it is advisable to pass from the circ function to some smoothed profile in which the transition from light to darkness occurs in a continuous way. Many different field profiles exhibit such a property, which is generally lost upon propagation. An example is furnished by super-Gaussian profiles,[14] whose use in laser cavities and other applications has given good results.[4,15–20] The study of the propagation features of the beams generated by these profiles is to be handled numerically.[14] A flattened profile giving rise to a field whose propagation is exactly known, at least under the paraxial approximation, could be attractive from a theoretical as well as from an applicative point of view, since it could permit better control of the beam characteristics.

In Ref. 21 a new class of axially symmetric coherent beams, the so-called flattened Gaussian beams (FGB's), was introduced. Their amplitude distribution across the waist plane is similar to that of a Gaussian beam whose central region has been flattened. The extension of the area in which the amplitude is approximately uniform is governed by an integer parameter, say, N. Although for small values of N the amplitude profile of a FGB is not very different from that of a Gaussian beam, it tends to a circ function for increasing values of N.

In this paper we describe the main properties of FGB's, concerning paraxial and far-field propagation, that make them an attractive alternative to other types of flattened beams. In particular, we give analytical expressions for the on-axis intensity and the far-field distribution and an asymptotic formula for the M^2 factor for large values of N. Furthermore, we report experimental investigations on their propagation features. It is to be noted that FGB's without axial symmetry, e.g., with a waist cross section resembling a rectangle, could be introduced.[21] In the present paper, however, we limit ourselves to the axially symmetric case.

2. GENERAL REMARKS

To understand how the analytical expression of the amplitude of a FGB at its waist plane can be derived, we start from the function

$$f_N(\xi) = \exp(-\xi^2) \sum_{n=0}^{N} \frac{\xi^{2n}}{n!}. \tag{1}$$

It is evident that for $N = 0$, $f_N(\xi)$ reduces to the Gaussian function $\exp(-\xi^2)$ and that if $N \to \infty$, the series on the right-hand side of Eq. (1) tends to compensate the Gaussian term, and $f_N(\xi) \to 1$. Curves of $f_N(\xi)$ for different values of N are shown in Fig. 1. Since the transition to very small values of f_N is seen to occur for $\xi \approx \sqrt{N}$,[21] by multiplying the argument of Eq. (1) by a quantity that behaves like $\sqrt{N}$, one obtains a new function, whose support coincides approximately with the interval [0, 1]. More precisely, we define a FGB of order N and spot size w_0 as a beam that, at its waist plane, has the following field distribution:

0740-3232/96/071385-10$10.00

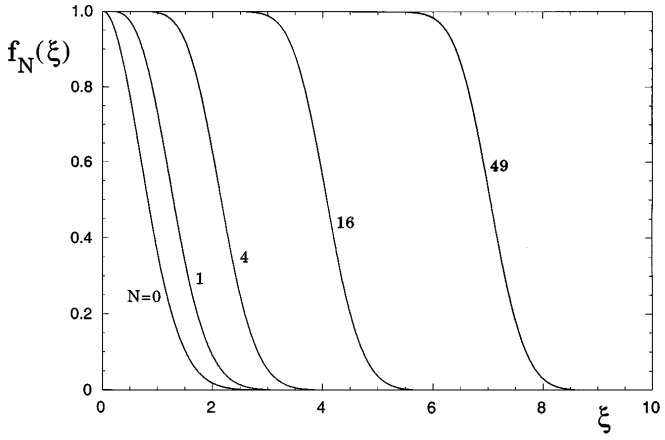

Fig. 1. Function f_N versus ξ [see Eq. (1)], for different values of N.

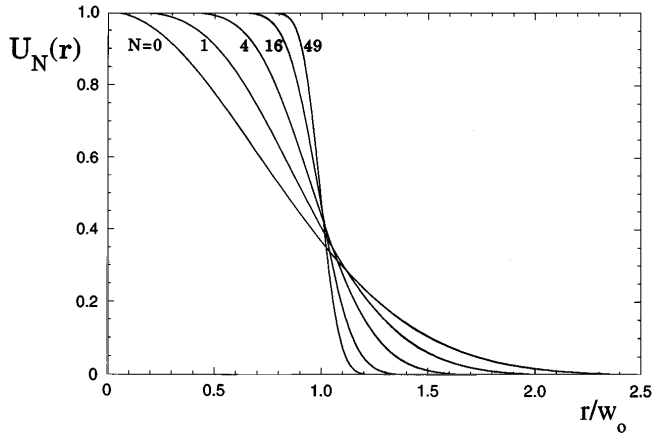

Fig. 2. Function U_N versus r [see Eq. (2)], for different values of N.

$$U_N(r) = A_0 f_N\left(\frac{\sqrt{N+1}\,r}{w_0}\right) = A_0 \exp\left[-\frac{(N+1)r^2}{{w_0}^2}\right] \sum_{n=0}^{N} \frac{1}{n!}\left(\frac{\sqrt{N+1}\,r}{w_0}\right)^{2n}, \quad (2)$$

where r is the radial coordinate, A_0 is a complex factor, and w_0 is a real quantity expressing the width of the beam.

On the basis of the previous considerations, a field of the type of Eq. (2) coincides with that of a Gaussian beam for $N = 0$, whereas it tends to the function $A_0\,\mathrm{circ}(r/w_0)$ when $N \to \infty$. It should be noted that in Ref. 21 the definition is slightly different, inasmuch as there the spatial variable r is scaled by $w_0/\sqrt{N}$ instead of $w_0/\sqrt{N+1}$. However, the present choice has the advantage that in this way the fundamental Gaussian beam is included in the class of Eq. (2) as the FGB of zero order. Of course, the two definitions tend to coincide when $N \gg 1$. The function $U_N(r)$ is shown in Fig. 2 as a function of r/w_0 for $A_0 = 1$ and different values of N.

Although FGB's form a discrete family, whereas, for example, super-Gaussian beams furnish a continuous set, it is seen from Eq. (2) as well as from Fig. 2 that, except for the first few values of N, FGB's afford a rather dense set for most practical purposes.

An estimate of the steepness of the function in the transition region can be obtained by evaluating the maximum absolute value of its derivative. In fact, since from Eq. (1) we have

$$f_N'(\xi) = -2\,\frac{\xi^{2N+1}}{N!}\exp(-\xi^2), \quad (3)$$

$$f_N''(\xi) = -2\,\frac{\xi^{2N}}{N!}(2N+1-2\xi^2)\exp(-\xi^2), \quad (4)$$

we can easily derive from Eq. (2) that the required maximum is

$$|U_N'|_{\max} = |A_0|\frac{2\sqrt{N+1}}{w_0 N!}\left(N+\frac{1}{2}\right)^{N+1/2} \times \exp\left[-\left(N+\frac{1}{2}\right)\right]. \quad (5)$$

For large values of N, the quantity $N!$ can be approximated by the Stirling formula[22] to obtain the result

$$|U_N'|_{\max} \simeq \frac{|A_0|}{w_0}\sqrt{\frac{2N}{\pi}}. \quad (6)$$

Relations (5) and (6) give the relationship between the order N of a FGB and its steepness, once A_0 and w_0 have been fixed.

In the case of a super-Gaussian profile of the form

$$V_\gamma(r) = A_0 \exp[-(r/w_0)^\gamma], \quad (7)$$

the same analysis leads to

$$|V_N'|_{\max} \simeq \frac{|A_0|}{w_0 e}\,\gamma\,; \quad (8)$$

i.e., its steepness is a linear function of the index γ. Approximations (6) and (8) suggest that for super-Gaussian profiles the index γ plays the same role as the square root of the order N of a FGB.

3. PARAXIAL PROPAGATION OF FLATTENED GAUSSIAN BEAMS

One of the most attractive advantages of using FGB's instead of other types of flattened beams consists in the fact that they can be easily expressed as a finite sum of Laguerre–Gauss beams.[23] In fact, as was shown in Ref. 21, the field in Eq. (2) can be written as

$$U_N(r) = A_0 \sum_{n=0}^{N} c_n^{(N)} L_n\left[\frac{2(N+1)r^2}{{w_0}^2}\right]\exp\left[-\frac{(N+1)r^2}{{w_0}^2}\right], \quad (9)$$

where L_n is the nth Laguerre polynomial[22] and

$$c_n^{(N)} = (-1)^n \sum_{m=n}^{N} \frac{1}{2^m}\binom{m}{n}. \quad (10)$$

From a computational point of view, the evaluation of the coefficients $c_n^{(N)}$ is made easier by the recurrence

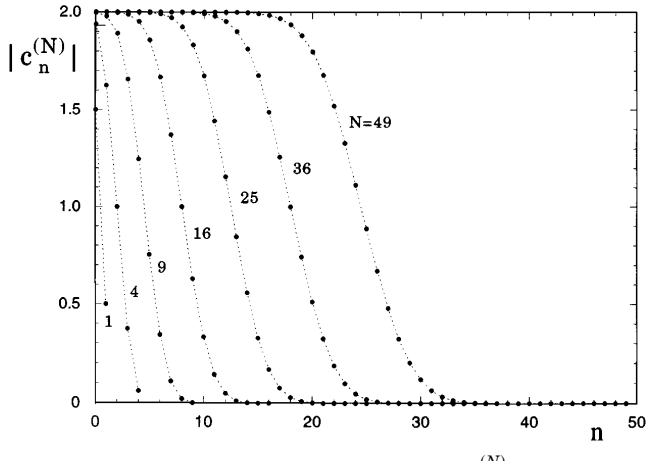

Fig. 3. Modula of the expansion coefficients $c_n^{(N)}$ for a FGB of order N [see Eq. (10)] versus n, for different values of N.

relation

$$c_{n+1}^{(N)} = -c_n^{(N)} + \frac{(-1)^n}{2^N}\binom{N+1}{n+1}, \qquad n = 0, \ldots, N-1,$$
$$c_0^{(N)} = 2 - 1/2^N, \tag{11}$$

and by the following symmetry property:

$$c_{N-n}^{(N)} = (-1)^{N-n}\left(2 - \left| c_n^{(N)} \right|\right), \tag{12}$$

whose proofs are reported in Appendix A. In Fig. 3 the modula of the coefficients $c_n^{(N)}$ for some values of N are shown. For the sake of clarity the (discrete) values of $c_n^{(N)}$ corresponding to each value of N have been linked by a dotted curve. It will be noticed that the law of variation of the $c_n^{(N)}$'s resembles the profile of the corresponding field distribution. This is reminiscent of the behavior of the eigenvalues of the prolate spheroidal wave functions[24] and of the underlying Szegö theorem.[25]

Once the $c_n^{(N)}$'s have been calculated, the problem of paraxial propagation of a FGB is solved by using the well-known propagation formulas of Laguerre–Gauss beams.[23] Therefore at a distance z from the waist plane we have

$$U_N(r; z) = A_0 \frac{w_N(0)}{w_N(z)} \exp\{i[kz - \Phi_N(z)]\} \times \exp\left\{\left[\frac{ik}{2R_N(z)} - \frac{1}{{w_N}^2(z)}\right] r^2\right\} \times \sum_{n=0}^{N} c_n^{(N)} L_n\left[\frac{2r^2}{{w_N}^2(z)}\right] \exp[-2in\Phi_N(z)], \tag{13}$$

where k is the wave number; w_N, R_N, and Φ_N are given by

$$w_N(z) = w_N(0)\sqrt{1 + \left[\frac{\lambda z}{\pi {w_N}^2(0)}\right]^2}, \tag{14a}$$

$$R_N(z) = z\left\{1 + \left[\frac{\pi {w_N}^2(0)}{\lambda z}\right]^2\right\}, \tag{14b}$$

$$\Phi_N(z) = \arctan\left[\frac{\lambda z}{\pi {w_N}^2(0)}\right]; \tag{14c}$$

and the spot size $w_N(0)$ of the Gaussian fields involved in expansion (9) is related to the width of the FGB through the relation

$$w_N(0) = \frac{w_0}{\sqrt{N+1}}. \tag{15}$$

In Fig. 4, plots of the intensity of propagated FGB's as a function of the radial coordinate r are shown for several values of z. In this figure $A_0 = 1$, $w_0 = 1$ mm, $\lambda = 0.5$ μm, and (a) $N = 4$, (b) $N = 16$, and (c) $N = 49$. Distances from the $z = 0$ plane are measured in terms of the Fresnel number,[11] which is defined as

$$N_F = {w_0}^2/\lambda z. \tag{16}$$

It can be noted that at $z \neq 0$ the transverse profile is no longer flat, owing to the dephasing of the component Laguerre–Gauss beams, and the typical structure of the Fresnel diffraction by circular aperture appears. This structure is more and more evident as N increases, so that we can say that the more the beam is flattened in its waist plane, the more its shape is distorted in propagation, as diffraction rings appear.

As in the case of Fresnel diffraction by a circular aperture, for a FGB, also, the on-axis intensity can be derived in a closed form. In fact, taking into account Eqs. (10) and (13), we have

$$\begin{aligned} U_N(0; z) &= A_0 \frac{w_N(0)}{w_N(z)} \exp\{i[kz - \Phi_N(z)]\} \times \sum_{n=0}^{N} c_n^{(N)} \exp[-2in\Phi_N(z)] \\ &= A_0 \frac{w_N(0)}{w_N(z)} \exp\{i[kz - \Phi_N(z)]\} \times \sum_{n=0}^{N} (-1)^n \sum_{m=n}^{N} \frac{1}{2^m}\binom{m}{n} \times \exp[-2in\Phi_N(z)], \end{aligned} \tag{17}$$

and, if we interchange the summation indexes and utilize Newton's binomial expansion,

$$\begin{aligned} U_N(0; z) &= A_0 \frac{w_N(0)}{w_N(z)} \exp\{i[kz - \Phi_N(z)]\} \times \sum_{m=0}^{N} \frac{1}{2^m} \sum_{n=0}^{m}\binom{m}{n} \times \{-\exp[-2i\Phi_N(z)]\}^n \\ &= A_0 \frac{w_N(0)}{w_N(z)} \exp\{i[kz - \Phi_N(z)]\} \times \sum_{m=0}^{N} \left\{\frac{1 - \exp[-2i\Phi_N(z)]}{2}\right\}^m. \end{aligned} \tag{18}$$

Finally, the sum in Eq. (18) is easily evaluated, yielding

$$U_N(0; z) = A_0 \frac{w_N(0)}{w_N(z)} \exp\{i[kz - \Phi_N(z)]\} \times \frac{1 - \sin^{N+1} \Phi_N(z) \exp\{-i(N+1)[\Phi_N(z) - \pi/2]\}}{\cos \Phi_N(z) \exp[-i\Phi_N(z)]}. \tag{19}$$

Hence, as far as the on-axis intensity is concerned, we can write

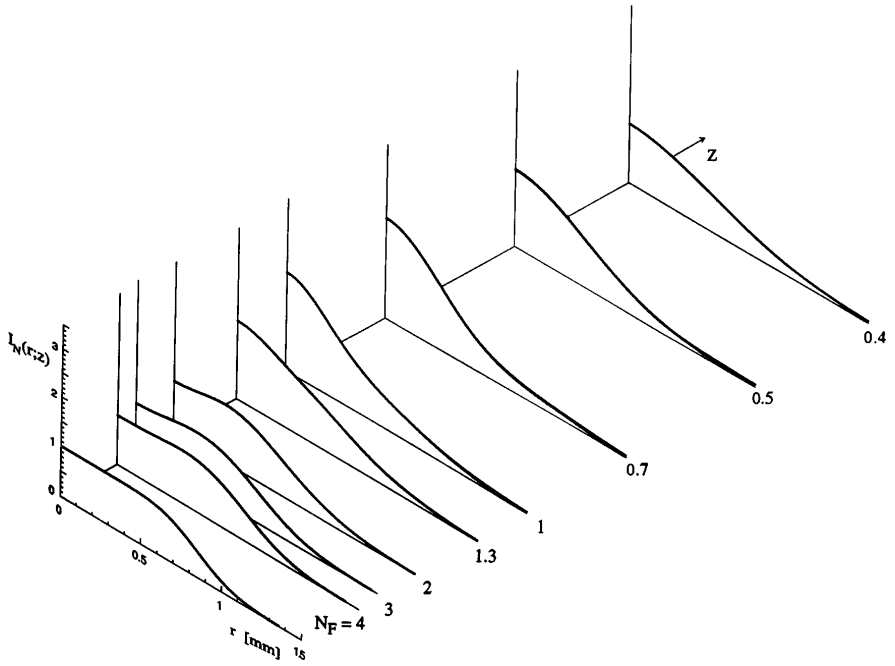

(a)

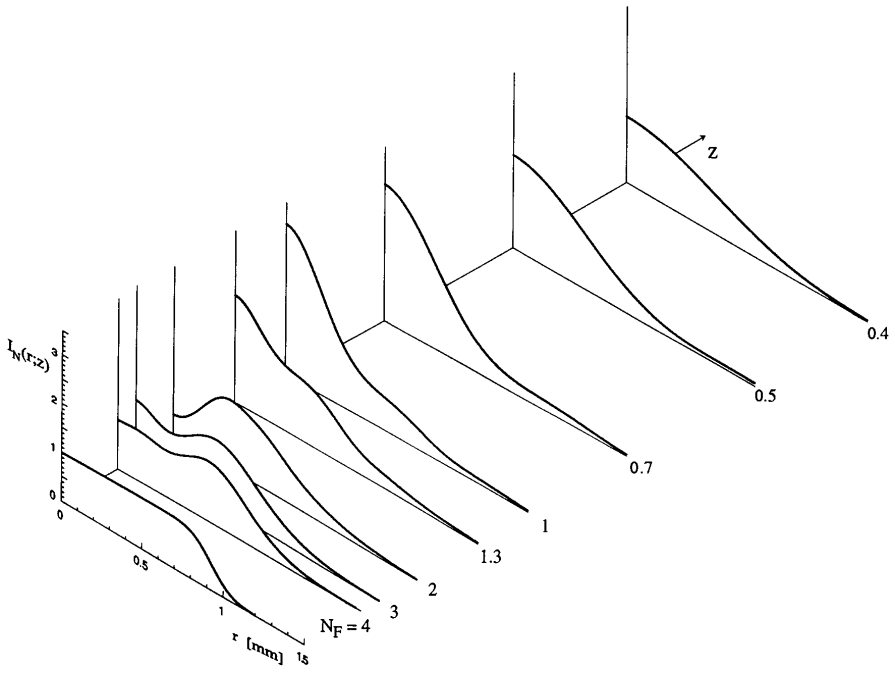

(b)

Fig. 4. Continues on facing page.

$$I_N(0; z) = |A_0|^2 \frac{{w_N}^2(0)}{{w_N}^2(z)} \frac{1 + \sin^{2N+2} \Phi_N(z) - 2 \sin^{N+1} \Phi_N(z) \cos\{(N+1)[\Phi_N(z) - \pi/2]\}}{\cos^2 \Phi_N(z)}. \quad (20)$$

Plots of the intensity [Eq. (20)] as a function of z are shown in Fig. 5, for different values of N, with $A_0 = 1$, $w_0 = 1$ mm, and $\lambda = 0.5$ μm. In particular, the presence of maxima and minima can be noted, in correspondence to odd and even values, respectively, of the Fresnel number. When N increases, the number of maxima and minima increases too, together with their sharpness, and the curves tend to the function

$$I_\infty(0; z) = 4|A_0|^2 \sin^2(k{w_0}^2/4z), \quad (21)$$

corresponding to the on-axis intensity for the case of a circular aperture.[11] In Fig. 5 this function is shown by means of a dotted curve. One can obtain expression (21)

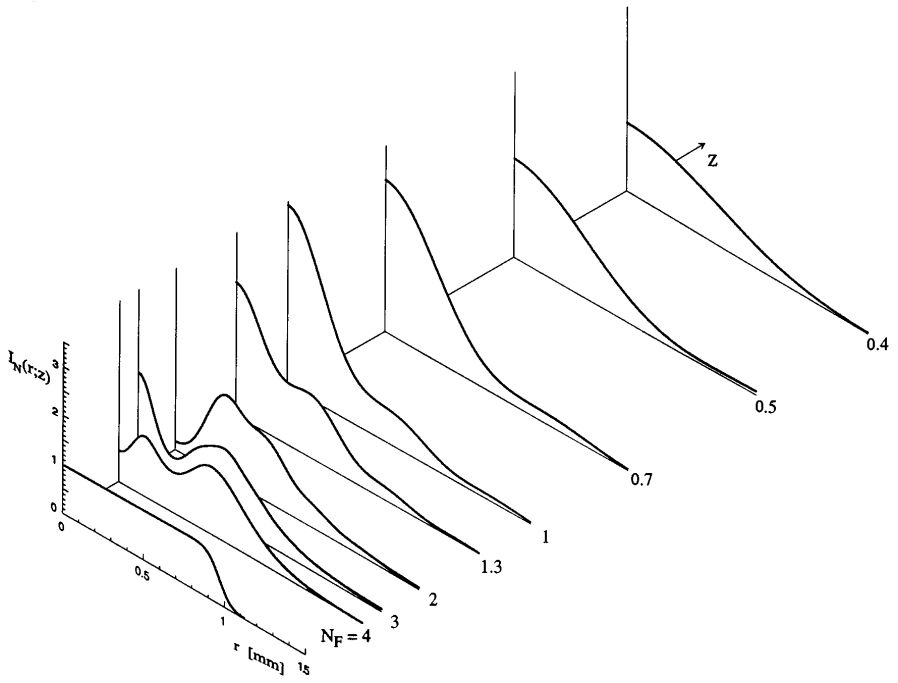

(c)

Fig. 4. Three-dimensional plots of the intensity of propagated FGB as a function of r and N_F, for (a) $N = 4$, (b) $N = 16$, and (c) $N = 49$. The other parameters are $w_0 = 1$ mm and $\lambda = 0.5$ μm.

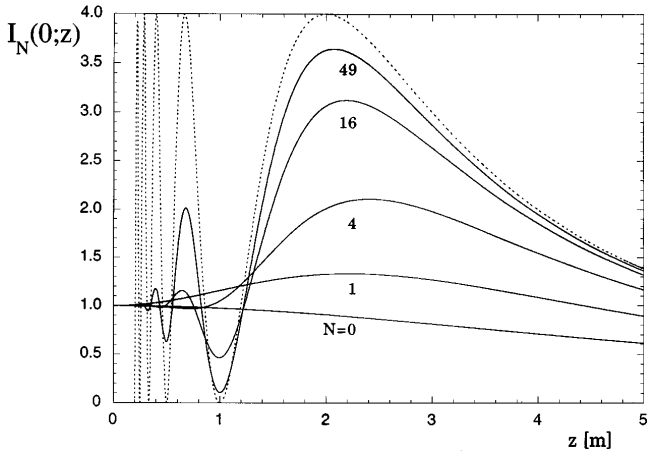

Fig. 5. FGB on-axis intensity as a function of z [see Eq. (20)], for different values of N (solid curves). The dotted curve represents the on-axis intensity associated with a circular hole of radius w_0 [see Eq. (16)]. The other parameters are $w_0 = 1$ mm and $\lambda = 0.5$ μm.

by evaluating the limit (for $N \to \infty$) of Eq. (20), taking into account Eqs. (14a) and (14c).

We note that the curves of the propagated intensity of a FGB are very similar to those reported in Ref. 14 for super-Gaussian beams, where results of numerical calculations are shown.

The propagation of a FGB through a general paraxial system may be studied as well, by use of the *ABCD* matrix formalism.[23] The result has the form of Eq. (13), where in $\exp(ikz)$ z is replaced by l, i.e., the optical path of a ray lying on the axis of the system, and Eqs. (14a)–(14c) are replaced by

$$w_N = A w_N(0) \sqrt{1 + [F(A, B)]^2}\,. \tag{22a}$$

$$R_N = AB\,\frac{1 + [F(A, B)]^{-2}}{1 + BC\{1 + [F(A, B)]^{-2}\}}\,, \tag{22b}$$

$$\Phi_N = \arctan[F(A, B)]\,, \tag{22c}$$

where $F(A, B) = \lambda B / A\pi w_N^2(0)$, A, B, C being matrix elements of the overall system. In the evaluation of Eqs. (22a)–(22c), for the sake of simplicity the input plane is assumed to be the waist plane of the beam. Furthermore, the relationship $AD - BC = 1$, which holds for any complex cascaded paraxial system, is used.

4. FAR-FIELD ANALYSIS AND THE M^2 FACTOR

Another useful property of a FGB is the fact that its Fourier transform can be expressed in a closed form, and therefore its far-field amplitude can be given in a simple way. Let $\tilde{U}_N(\rho)$ be the Hankel transform of zero order[26] of $U_N(r)$; i.e.,

$$\begin{aligned}\tilde{U}_N(\rho) &= 2\pi \int_0^\infty U_N(r) J_0(2\pi\rho r) r\,\mathrm{d}r \\ &= 2\pi \sum_{n=0}^{N} \frac{\alpha^n}{n!} \int_0^\infty r^{2n+1} J_0(2\pi\rho r) \\ &\quad \times \exp(-\alpha r^2)\mathrm{d}r\,,\end{aligned} \tag{23}$$

where, for the sake of brevity, we set

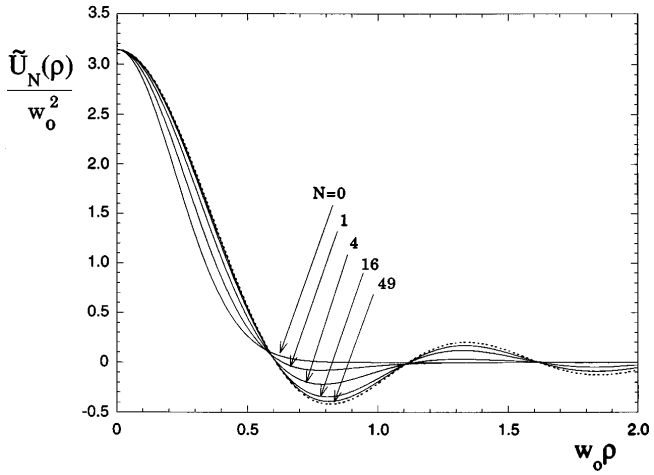

Fig. 6. Two-dimensional Fourier transform of function $U_N(r)$ [see Eq. (26)] normalized to the value $w_0{}^2$, for different values of N. The dotted curve represents a two-dimensional Fourier transform of circ(r/w_0) [see Eq. (28)].

$$\alpha = \frac{N+1}{w_0{}^2}, \tag{24}$$

and J_0 is the zero-order Bessel function of the first kind. The integrals in the sum of Eq. (23) can be evaluated,[27] giving

$$\tilde{U}_N(\rho) = \frac{\pi}{\alpha}\exp\left(-\frac{\pi^2}{\alpha}\rho^2\right)\sum_{n=0}^{N} L_n\left(\frac{\pi^2}{\alpha}\rho^2\right), \tag{25}$$

and, from properties of Laguerre polynomials,[27] we obtain

$$\begin{aligned}\tilde{U}_N(\rho) &= \frac{\pi}{\alpha}\exp\left(-\frac{\pi^2}{\alpha}\rho^2\right)L_n^{(1)}\left(\frac{\pi^2}{\alpha}\rho^2\right)\\ &= \frac{\pi w_0{}^2}{N+1}L_n^{(1)}\left(\frac{\pi^2 w_0{}^2}{N+1}\rho^2\right)\exp\left(-\frac{\pi^2 w_0{}^2}{N+1}\rho^2\right),\end{aligned} \tag{26}$$

where $L_n^{(1)}$ is the generalized Laguerre polynomial with indices N and 1, and use has been made of Eq. (24). In Fig. 6, plots of $\tilde{U}_N(\rho)/w_0{}^2$ for different values of N are shown.

Finally, it is possible to show that Eq. (26) gives the field diffracted by a circular aperture when N goes to infinity. In fact, since[22]

$$\lim_{n\to\infty}\left[\frac{1}{n^\beta}L_n^{(\beta)}\left(\frac{x}{n}\right)\right] = x^{-\beta/2}J_\beta(2\sqrt{x}), \tag{27}$$

then

$$\lim_{N\to\infty}\tilde{U}_N(\rho) = \frac{J_1(2\pi w_0\rho)}{\rho}w_0, \tag{28}$$

which coincides with the two-dimensional Fourier transform of circ(r/w_0).[11] In Fig. 6 this limiting behavior is shown by means of a dotted curve. It can be seen that in the central zone the spectrum is well approximated by the limiting curve even for small values of N, whereas the difference becomes more and more evident as the radial coordinate increases. In particular, for any finite N, the corresponding curves decrease more rapidly than in the limiting case. As we shall see in the following, such behavior accounts for the finite width of the far-field distribution of a FGB.

One of the most important parameters in studying a light beam is the so-called M^2 factor,[28,29] which is a quality factor indicating the diverging attitude of a beam, once its spot size at the waist, i.e., its minimum width, has been fixed. It can be proved that, for a fixed spot size at the waist, the less diverging beam is a Gaussian beam of zero order. Accordingly, M^2 measures the difference in diffractive spread between a general beam (whose M^2 is always >1) and a Gaussian one ($M^2 = 1$).

If $U(r)$ represents the disturbance on the waist plane of a general, circularly symmetric beam and $\tilde{U}(\rho)$ is its Hankel transform of zero order, then M^2 is defined as

$$M^2 = 2\pi\sigma_r\sigma_\rho, \tag{29}$$

where

$$\sigma_r{}^2 = \frac{\int_0^\infty |U(r)|^2 r^3 \mathrm{d}r}{\int_0^\infty |U(r)|^2 r\mathrm{d}r}, \tag{30}$$

$$\sigma_\rho{}^2 = \frac{\int_0^\infty |\tilde{U}(\rho)|^2 \rho^3 \mathrm{d}\rho}{\int_0^\infty |\tilde{U}(\rho)|^2 \rho\mathrm{d}\rho}. \tag{31}$$

In the case of a FGB, the quantities in Eqs. (30) and (31) can be evaluated starting from Eqs. (2) and (26). In the following we shall use the quantities R_N, s_N, and T_N, which are defined through the relations

$$\int_0^\infty |U_N(r)|^2 r^3 \mathrm{d}r = |A_0|^2 \frac{w_0{}^4}{8(N+1)^2}R_N, \tag{32}$$

$$\int_0^\infty |\tilde{U}_N(\rho)|^2 \rho^3 \mathrm{d}\rho = |A_0|^2 S_N, \tag{33}$$

$$\begin{aligned}\int_0^\infty |U_N(r)|^2 r\mathrm{d}r &= \int_0^\infty |\tilde{U}_N(\rho)|^2 \rho\mathrm{d}\rho\\ &= |A_0|^2 \frac{w_0{}^2}{4(N+1)}T_N,\end{aligned} \tag{34}$$

the identity of the two integrals in Eq. (34) being ensured by Parseval's theorem.[26] With these definitions, variances (30) and (31) can be written as

$$\sigma_r{}^2 = \frac{w_0{}^2}{2(N+1)}\frac{R_N}{T_N}, \tag{35}$$

$$\sigma_\rho{}^2 = \frac{4(N+1)}{w_0{}^2}\frac{S_N}{T_N}; \tag{36}$$

hence

$$M^2 = 2\pi\frac{\sqrt{2R_N S_N}}{T_N}. \tag{37}$$

The quantity S_N can be given the simple form

$$S_N = \frac{1}{4\pi^2}\frac{(2N+1)!}{(N!)^2 2^{2N+1}}, \tag{38}$$

if we perform some calculations that make use of results

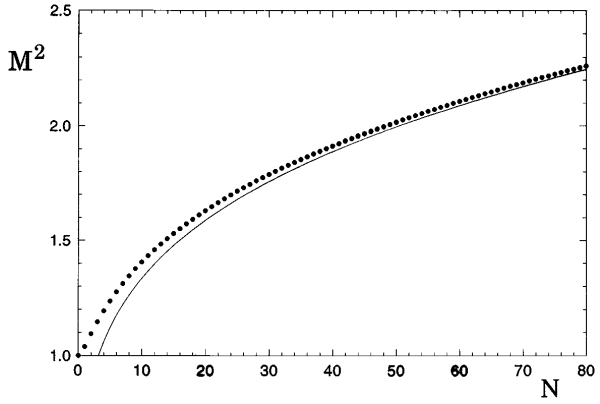

Fig. 7. Behavior of the M^2 quality factor for a FGB as a function of N. Dotted curve, exact values [Eq. (41)]; solid curve, approximation (45).

contained in Ref. 27; and for R_N and T_N, expressions in terms of finite sums can be obtained:

$$R_N = \sum_{n=0}^{N} \sum_{m=0}^{N} \frac{n+m+1}{2^{n+m}} \binom{n+m}{n}, \tag{39}$$

$$T_N = \sum_{n=0}^{N} \left[\sum_{m=n}^{N} \frac{1}{2^m} \binom{m}{n} \right]^2. \tag{40}$$

In conclusion, the M^2 factor of a FGB turns out to be

$$M^2 = \frac{2^{-N}}{N!\,T_N} \sqrt{(2N+1)!\,R_N}\,. \tag{41}$$

Figure 7 (dotted curve) shows the M^2 values calculated with Eqs. (39)–(41). It can be seen that, starting from the value 1 for $N = 0$, M^2 increases monotonically as a function of N, according to the fact that definition (29) furnishes an infinite value in the case of fields exhibiting discontinuities.[30]

Since Eq. (41) involves double sums (39) and (40), the evaluation of the quality factor of a FGB is a bit tedious for large N. Although such an evaluation is to be made once and for all because M^2 does not depend on w_0, it is worthwhile to give a rough estimate of M^2 for large values of N. In fact, in such a case $U_N(r)$ can be approximated by the function $\mathrm{circ}(r/w_0)$ in the evaluation of integrals (32) and (34). So we get

$$R_N \simeq \frac{8N^2}{{w_0}^4} \int_0^{w_0} r^3 \mathrm{d}r = 2N^2, \tag{42}$$

$$T_N \simeq \frac{4N}{{w_0}^2} \int_0^{w_0} r \mathrm{d}r = 2N, \tag{43}$$

and, from Eq. (41),

$$M^2 \simeq \frac{\sqrt{(2N+1)!}}{2^{N+1/2} N!}\,. \tag{44}$$

Finally, by using Stirling's formula for the evaluation of the factorials in Eq. (44), we obtain the asymptotic expression

$$M^2 \approx (N/\pi)^{1/4}. \tag{45}$$

The corresponding curve is drawn in Fig. 7 as a solid curve. The agreement between exact and approximated values is good not only for large N, as could be expected, but even for relatively small N. For example, the relative error does not exceed 5% for $N > 10$.

In Ref. 14 the limiting value of M^2 for a super-Gaussian beam is shown to be

$$M^2 \approx \sqrt{\gamma}/2\,. \tag{46}$$

On comparing relations (45) and (46) we note that, as far as the divergence is concerned, a FGB of order N behaves like a super-Gaussian beam with a parameter γ proportional to $\sqrt{N}$. This remark agrees with the one made at the end of Section 2.

5. EXPERIMENT

In order to verify the practical feasibility of fields exhibiting the behavior described in the previous sections, we generated a FGB by illuminating an amplitude transparency by a suitably expanded and collimated laser beam and investigated some of its propagation features in both the near and the far field.

The transparency was implemented by photographing a computer monitor, where an intensity profile proportional to $U_N(r)$, given by Eq. (2), was visualized. The photographic medium consisted of a holographic plate Agfa Holotest 8E56. Because of possible nonlinearities in the emulsion response, some care must be used in this process, and the obtained values of N and w_0 are to be checked *a posteriori,* by measuring the transmittivity profile of the obtained transparency. An example is shown in Fig. 8, where experimental values (circles) are drawn together with the best-fitting curve (solid curve). The fit leads to $N = 14$, $w_0 = 0.53$ mm.

To investigate the propagation of a FGB, we illuminated such a transparency by a suitably expanded and spatially filtered beam produced by an Argon laser operating at wavelength $\lambda = 514.5$ nm. The near-field propagated intensity was then measured, by means of a linear CCD detector, on the planes $z = 182$ mm, $z = 273$ mm, and $z = 546$ mm, corresponding to Fresnel numbers 3, 2, and 1, respectively. The observed patterns showed a certain lack of circular symmetry, presumably owing to imperfections of the plate supporting the amplitude transparency. The measured values, represented by circles, are shown in Fig. 9 along with the theoretical values (solid curves), which we obtained by using Eq. (13), with the actual values as parameters. In each case the reported experimental values refer to the diame-

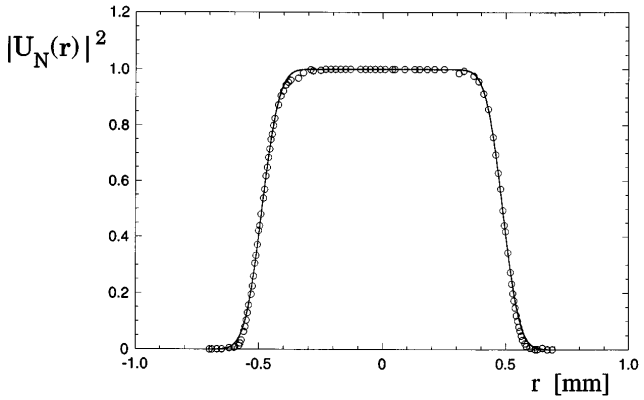

Fig. 8. Experimental values (circles) of intensity profile for a FGB on its waist plane, with $N = 14$ and $w_0 = 0.53$ mm. The solid curve indicates the theoretical curve $|U_N(r)|^2$.

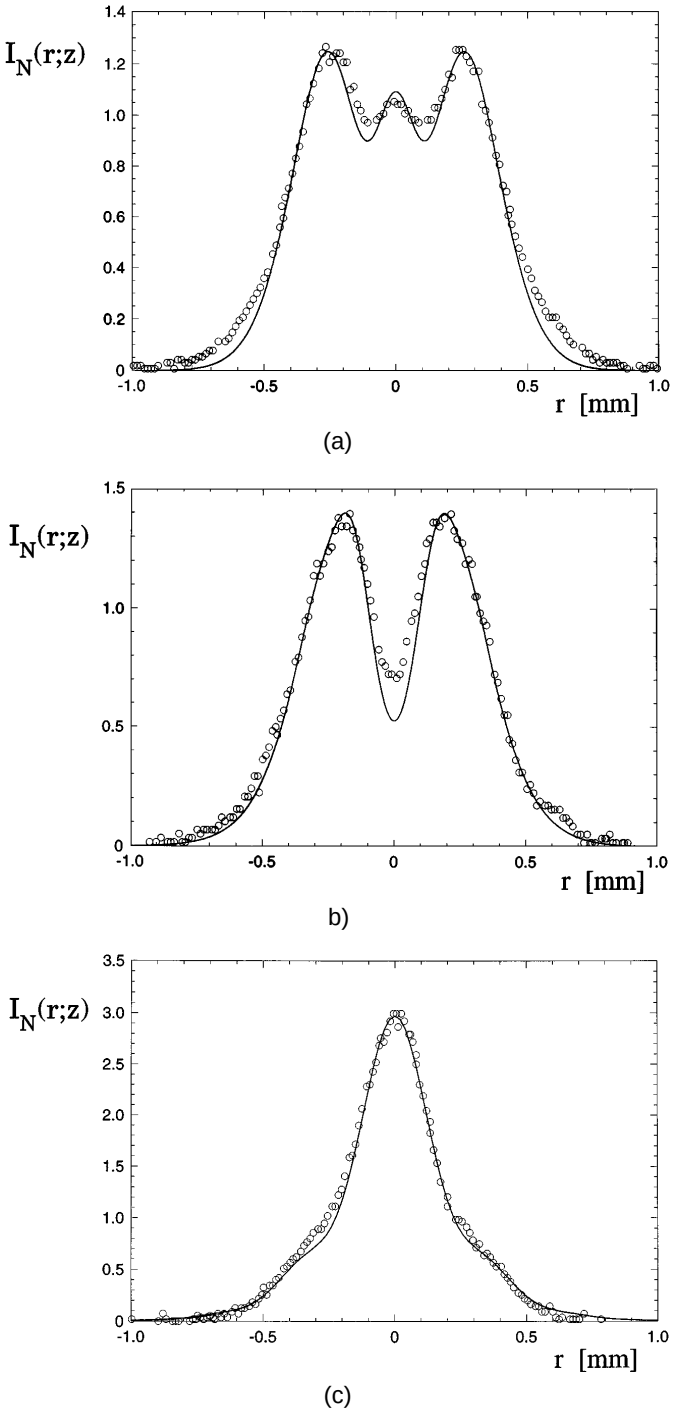

Fig. 9. Experimental near-field propagated intensity profile of the FGB of Fig. 8 (circles) at (a) $z = 182$ mm, (b) $z = 273$ mm, and (c) $z = 546$ mm. Solid curves indicate the theoretical behavior as predicted by Eq. (13).

ter along which the agreement between theory and experiment is best. Arbitrary units are used for the vertical axis. In Figs. 10(a), 10(b), 10(c), and 10(d), photographs of the cross section of the FGB are shown, taken in the planes $z = 0$, $z = 182$ mm, $z = 273$ mm, and $z = 546$ mm, respectively.

Figure 11 shows, in arbitrary units, intensity values along the propagation axis, both experimental (circles) and predicted by Eq. (20) (solid curve).

Finally, Fig. 12 shows the far-field intensity profile. Circles represent measured values, and the solid curve is the theoretical curve derived from Eq. (26). The far-field condition was obtained by means of a converging lens. Since a magnification of the focal-plane image was used, the radial coordinate is measured in arbitrary units and does not reproduce the real beam dimension. The beam cross section in the far field is shown in Fig. 13. Note that in this picture the central zone has been deliberately saturated in order to exhibit the presence of the first diffraction ring, which is actually much less intense than the central lobe, as can be seen in Fig. 12. The number of practically observable diffraction rings is lower than in the case of a circular hole, as was pointed out in Section 4.

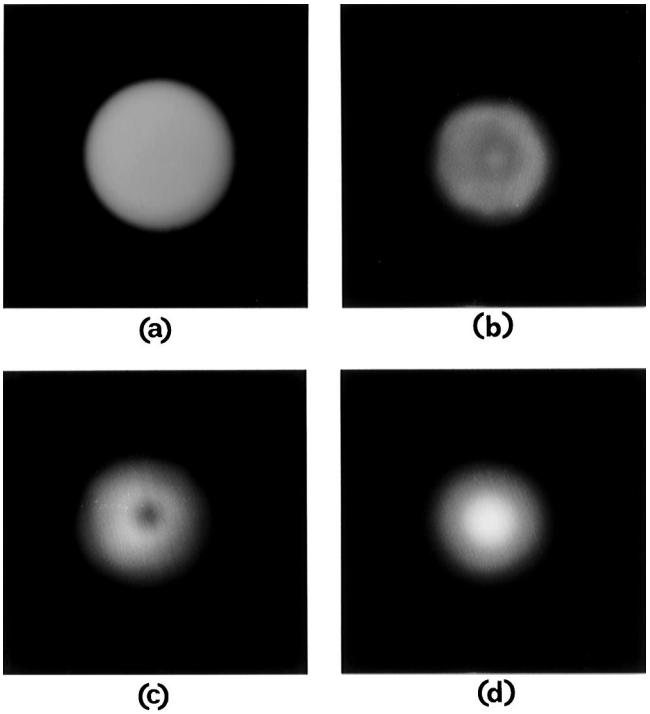

Fig. 10. Experimental transverse distributions of the intensity of the FGB of Fig. 8 at (a) $z = 0$, (b) $z = 182$ mm, (c) $z = 273$ mm, and (d) 546 mm.

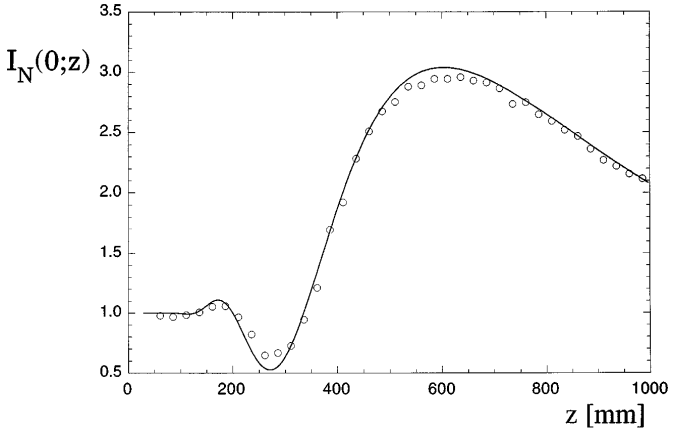

Fig. 11. Experimental behavior of on-axis intensity of the FGB of Fig. 8 (circles), together with the theoretical behavior (solid curve) as predicted by Eq. (20).

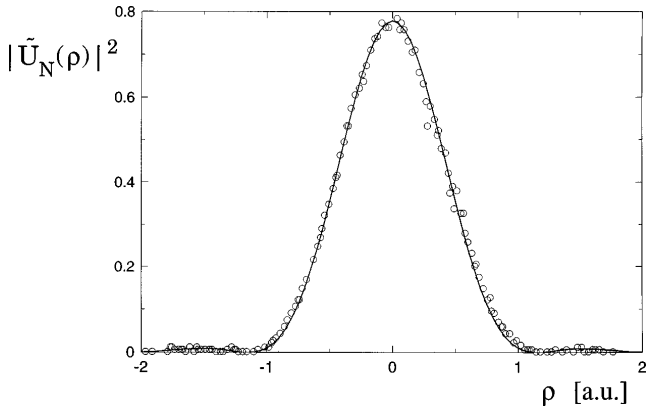

Fig. 12. Experimental far-field intensity profile of the FGB of Fig. 8 (circles), together with the theoretical behavior (solid curve) as predicted by Eq. (26).

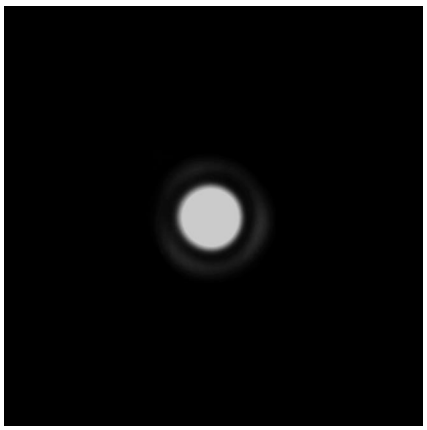

Fig. 13. Experimental transverse distribution of the far-field intensity of the FGB of Fig. 8.

6. CONCLUSIONS

FGB's seem to offer a convenient answer to a recurrent question: Which mathematical model should we use to describe a field distribution that at some waist plane is uniphase and nearly flat within a disk and passes to zero in a continuous and nonoscillatory way? The question of course is to be specified by some requirement. In fact, although there are an infinite number of possible formulas representing such a type of field, a desirable feature would be the ability of evaluating in an easy way the corresponding field distribution everywhere in space upon free propagation. From this standpoint some widely used profiles such as the super-Gaussian are not entirely satisfactory, because the corresponding propagation problem is to be treated numerically. FGB's, on the other hand, reduce the propagation problem to the simple task of summing up N Laguerre–Gauss modes. We have seen in this paper that for some quantities of interest, such as the axial intensity and the far-field distribution, even simpler results are obtained. We have also seen that FGB's are easily synthesized in the laboratory with the use of pure amplitude transparencies so that no phase control techniques are required. A final question could be as follows: Is the waist profile of a FGB less convenient than other profiles for modeling features of actual optical devices such as variable reflectivity mirrors with flat top? The answer is negative. As clarified by a recent investigation,[31] the FGB profile is so similar to, for example, a super-Gaussian profile that the two can fit the experimental data with comparable accuracy.

7. APPENDIX A: SOME USEFUL PROPERTIES OF $c_n^{(N)}$ COEFFICIENTS

Let us start from Eq. (10), written for $n+1$:

$$c_{n+1}^{(N)} = (-1)^{n+1} \sum_{m=n+1}^{N} \frac{1}{2^m} \binom{m}{n+1}. \tag{A1}$$

Setting $m-1=k$, we get

$$c_{n+1}^{(N)} = \frac{(-1)^{n+1}}{2} \sum_{k=n}^{N-1} \frac{1}{2^k} \binom{k+1}{n+1}, \tag{A2}$$

and, using the well-known property of the binomial coefficients,

$$\binom{k+1}{n+1} = \binom{k}{n} + \binom{k}{n+1}, \tag{A3}$$

we obtain

$$c_{n+1}^{(N)} = \frac{(-1)^{n+1}}{2} \left[\sum_{k=n}^{N-1} \frac{1}{2^k} \binom{k}{n} + \sum_{k=n+1}^{N-1} \frac{1}{2^k} \binom{k}{n+1} \right]. \tag{A4}$$

Result (A4) may be written in the form

$$\begin{aligned} c_{n+1}^{(N)} &= -\frac{1}{2} \left\{ (-1)^n \sum_{k=n}^{N} \frac{1}{2^k} \binom{k}{n} - (-1)^{n+1} \sum_{k=n+1}^{N} \frac{1}{2^k} \binom{k}{n+1} \right. \\ &\quad \left. - \frac{(-1)^n}{2^N} \left[\binom{N}{n} + \binom{N}{n+1} \right] \right\} \\ &= -\frac{1}{2} \left[c_n^{(N)} - c_{n+1}^{(N)} - \frac{(-1)^n}{2^N} \binom{N+1}{n+1} \right], \end{aligned} \tag{A5}$$

where property (A3) has been used again. Equation (11) follows immediately from Eq. (A5) and enables one to evaluate all the $c_n^{(N)}$ coefficients starting from $c_0^{(N)}$, whose value,

$$c_0^{(N)} = 2 - \frac{1}{2^N}, \tag{A6}$$

is easily calculated by Eq. (10).

The evaluation of $c_N^{(N)}$ is straightforward, too, and the result is

$$c_N^{(N)} = \frac{(-1)^N}{2^N}, \tag{A7}$$

so that

$$\left| c_0^{(N)} \right| + \left| c_N^{(N)} \right| = 2. \tag{A8}$$

This result is generalized by induction; i.e., it is easy to prove that, if

$$\left| c_{n-1}^{(N)} \right| + \left| c_{N-n+1}^{(N)} \right| = 2, \tag{A9}$$

then

$$\left| c_n^{(N)} \right| + \left| c_{N-n}^{(N)} \right| = 2. \tag{A10}$$

According to Eq. (11), we have

$$
\begin{aligned}
&\left| c_n^{(N)} \right| + \left| c_{N-n}^{(N)} \right| \\
&\quad = (-1)^n c_n^{(N)} + (-1)^{N-n} c_{N-n}^{(N)} \\
&\quad = (-1)^n \left[-c_{n-1}^{(N)} + \frac{(-1)^{n-1}}{2^N} \binom{N+1}{n} \right] \\
&\qquad + (-1)^{N-n} \left[-c_{N-n+1}^{(N)} + \frac{(-1)^{N-n}}{2^N} \binom{N+1}{N-n+1} \right] \\
&\quad = \left| c_{n-1}^{(N)} \right| + \left| c_{N-n+1}^{(N)} \right| \\
&\qquad + \frac{1}{2^N} \left[\binom{N+1}{N+1-n} - \binom{N+1}{n} \right] \\
&\quad = \left| c_{n-1}^{(N)} \right| + \left| c_{N-n+1}^{(N)} \right|, \qquad \text{(A11)}
\end{aligned}
$$

since the term in the square brackets vanishes.

ACKNOWLEDGMENTS

The authors thank Silvia Vicalvi and Fulvio Medici for their helpful contributions. This research is supported by Ministero dell'Università e della Ricerca Scientifica e Tecnologica and Istituto Nazionale di Fisica della Materia.

REFERENCES AND NOTES

1. C. S. Ih, "Absorption lens for producing uniform laser beams," Appl. Opt. **11,** 694–697 (1972).
2. P. E. Klingsporn, "Theoretical intensity uniformity from an anti-Gaussian collimating lens," Appl. Opt. **15,** 2355–2357 (1976).
3. Y. Kawamura, Y. Itagaki, K. Toyota, and S. Namba, "A simple optical device for generating square flat-top intensity irradiation from a Gaussian laser beam," Opt. Commun. **48,** 44–46 (1983).
4. S. De Silvestri, P. Laporta, V. Magni, and O. Svelto, "Solid-state laser unstable resonators with tapered reflectivity mirrors: the super-Gaussian approach," IEEE J. Quantum Electron. **24,** 1172–1177 (1988).
5. V. Kermene, A. Saviot, M. Vampouile, B. Colombeau, C. Froehly, and T. Dohnalik, "Flattening of the spatial laser beam profile with low losses and minimal beam divergence," Opt. Lett. **17,** 859–862 (1992).
6. S. K. Dew and R. R. Parsons, "Absorbing filter to flatten Gaussian beams," Appl. Opt. **31,** 3416–3419 (1992).
7. A. J. Cox and J. D'Anna, "Constant-axial-intensity nondiffracting beam," Opt. Lett. **17,** 232–234 (1992).
8. P. H. Malyak, "Two-mirror unobscured optical system for reshaping the irradiance distribution of a laser beam," Appl. Opt. **31,** 4377–4383 (1992).
9. C. Xie, R. Gupta, and H. Metcalf, "Beam profile flattener for Gaussian beams," Opt. Lett. **18,** 173–175 (1993).
10. As usual, circ(r) is defined as 1 if $r \leq 1$ and 0 elsewhere, r being the radial coordinate in R^2.
11. M. Born and E. Wolf, *Principles of Optics,* 6th ed., reprinted (Pergamon, Oxford, 1993).
12. R. Barakat, "The calculation of integrals encountered in optical diffraction theory," in *The Computer in Optical Research,* B. R. Frieden, ed. (Springer-Verlag, Berlin, 1980), pp. 35–80.
13. C. J. R. Sheppard and M. Hrynevych, "Diffraction by a circular aperture: a generalization of Fresnel diffraction theory," J. Opt. Soc. Am. A **9,** 274–281 (1992).
14. A. Parent, M. Morin, and P. Lavigne, "Propagation of super-Gaussian field distributions," Opt. Quantum Electron. **24,** 1071–1079 (1992).
15. M. S. Bowers, "Diffractive analysis of unstable optical resonators with super-Gaussian mirrors," Opt. Lett. **19,** 1319–1321 (1992).
16. P. A. Bélanger, R. L. Lachance, and C. Paré, "Super-Gaussian output from a CO_2 laser by using a graded-phase mirror resonator," Opt. Lett. **17,** 739–741 (1991).
17. M. R. Perrone, A. Piegari, and S. Scaglione, "On the super-Gaussian unstable resonators for high-gain short-pulse laser media," IEEE J. Quantum Electron. **29,** 1423–1427 (1993).
18. G. Duplain, P. G. Verly, J. A. Dobrowolski, A. Waldorf, and S. Bussière, "Graded-reflectance mirrors for beam quality control in laser resonators," Appl. Opt. **32,** 1145–1153 (1993).
19. J. Ojeda-Castañeda, G. Saavedra, and E. López-Olazagasti, "Super-Gaussian beams of continuous order as GRIN modes," Opt. Commun. **102,** 21–24 (1993).
20. S. Bollanti, P. Di Lazzaro, F. Flora, G. Giordano, T. Letardi, C. Petrucci, G. Schina, and C. E. Zheng, "Compact three-electrodes excimer laser IANUS for a POPA optical system," in *High-Power Gas and Solid State Lasers,* D. Schuoecker, T. Letardi, M. Bohrer, and H. Weber, eds., Proc. SPIE **2206,** 144–153 (1994).
21. F. Gori, "Flattened Gaussian beams," Opt. Commun. **107,** 335–341 (1994).
22. M. Abramowitz and I. Stegun, eds., *Handbook of Mathematical Functions* (Dover, New York, 1972).
23. A. E. Siegman, *Lasers* (University Science, Mill Valley, Calif., 1986).
24. D. Slepian and H. O. Pollak, "Prolate spheroidal wave functions: Fourier analysis and uncertainty. I," Bell Syst. Tech. J. **40,** 43–63 (1961).
25. H. J. Landau, "On Szegö eigenvalue distribution theorem and non-Hermitian kernels," J. Analyse Math. **28,** 335–357 (1975).
26. R. N. Bracewell, *The Fourier Transform and Its Applications,* 2nd ed., revised (McGraw-Hill, New York, 1986).
27. A. P. Prudnikov, Yu. A. Brychkov, and O. I. Marichev, *Integrals and Series.* Vol. I, reprinted (Gordon & Breach, New York, 1992).
28. A. E. Siegman, "New developments in laser resonators," in *Optical Resonators,* D. A. Holmes, ed., Proc. SPIE **1224,** 2–14 (1990).
29. J. Serna, P. M. Mejías, and R. Martínez-Herrero, "Beam quality changes in Hermite–Gauss mode fields propagating through Gaussian apertures," Appl. Opt. **32,** 1084–1086 (1993).
30. P.-A. Bélanger, Y. Champagne, and C. Paré, "Beam propagation factor of diffracted laser beams," Opt. Commun. **105,** 233–242 (1994).
31. C. Palma and V. Bagini, "Propagation of super-Gaussian beams," Opt. Commun. **111,** 6–10 (1994).